A non-defect precursor gate oxide breakdown model

Kin P. Cheung
National Institute of Standards & Technology, Gaithersburg, MD U.S.A. kin.cheung@nist.gov

Abstract: Understanding defect creation is central to efforts to comprehend gate dielectric breakdown in metal-oxide-semiconductor-field-effect-transistors (MOSFETs). While gate dielectrics other than SiO_2 are now popular, models develop for SiO_2 breakdown are used for these dielectrics too. Considering that the Si-O bond is very strong, modeling efforts have focused in ways to weaken it so that defect creation (bond-breaking) is commensurate with experimental observations. So far, bond-breaking models rely on defect-precursors to make the energetics manageable. Here it is argued that the success of the percolation model for gate oxide breakdown precludes the role of defect precursors in gate oxide breakdown. It is proposed that defect creation involves "normal" Si-O bonds. This new model relies on the fact that hole transport in SiO_2 is in the form of a small polaron – meaning that it creates a transient local distortion as it travels. It is this transient distortion that enables normal Si-O bonds to be weakened (albeit transiently) enough that breaking the bonds at a rate commensurate with measurements becomes possible without the help of the externally applied field.

Key words: gate oxide; breakdown; precursor; hole transport; small polaron; lone-pair; percolation model.

Introduction

Gate oxide breakdown has been an important topic ever since silicon-based integrated circuits dominated electronics. Tremendous work has been done to understand the breakdown mechanism as well as to project the breakdown lifetime at operation condition [1]. After decades of effort, progress has been made but important questions about the defect creation mechanism remain.

One of the most important advances in gate oxide breakdown research is the realization that breakdown is triggered by defects, accumulating under electrical stress, reaching a critical density [2-4]. This leads to the development of the percolation model [5-8] which successfully predicts the Weibull shape factor, β (slope of the Weibull plot), of the measured oxide breakdown distributions as a function of oxide thickness. The percolation model has become the most important tool for the projection of gate oxide breakdown reliability to operation conditions.

The percolation model assumes that, under the stress of an electric field E, defects are created at random locations within the oxide film. The probability of forming a percolation path (the initial conduction path of breakdown) with defects, for a given oxide thickness, is a unique function of the defect density and the effective defect size. In other words, for a given probability of breakdown, there is an associated critical defect density. It is quite clear that if the defect creation process were not random, a different statistical outcome will result (different set of β). The success of the percolation model is therefore a strong statement that defects are indeed created at random locations under electrical stress and places a strong constraint on any proposed defect creation mechanisms.

Depending on the device area and oxide thickness, the critical defect density to breakdown is predicted and experimentally demonstrated to reach beyond mid $10^{20}/cm^3$ [3, 7]. Defects are often thought to be created from precursors. In that case, a precursor depletion phenomenon (deviation from the prediction of the percolation model) should exist when the precursor density is limited. However, experimentally, the β for device areas down to sub-micron scales show no sign of deviation from the percolation model. (Smaller device areas lead to higher critical defect densities). Thus, if defects were created from precursor sites, the density of precursor sites must be over mid $10^{21}/cm^3$, or greater than 10% of the SiO_2 bond density. Based on this, Nissan-Cohen et al. concluded that defects (responsible for breakdown) cannot be created solely from precursor sites [3].

Difficulties of existing models

Among gate oxide degradation models, the thermochemical model (E model) considers defect creation by direct bond-breaking through the molecular dipole-electric field interaction [9]. The strongest support for this first order kinetic model is that it can fit the experimentally measured [10] field acceleration factor and thermal activation energy. However, it predicts that only the precursor weakened bonds (oxygen vacancies) can be broken to produce defects. Also, this model cannot reconcile with the overwhelming experimental observations that tunneling current plays a strong role in breakdown lifetime [3, 4, 11, 12].

The competing anode-hole injection model (*1/E* model) [13-16] posits that hot holes are created by electrons arriving at the anode and that some of these hot holes can tunnel back into the oxide, leading to defect creation by an unknown process. This model can explain the role of tunneling current in breakdown but cannot explain the temperature-dependence of breakdown. Since tunneling current is flowing in all the oxide breakdown experiments, the anode-hole injection model is widely accepted. Its popularity continues even after the strongest supporting evidence of the model, the critical hole-fluence to breakdown [14], is proven to be a misinterpretation of the experiment [17]. This is, in part, because the evidence of hole-trapping during electrical stress is overwhelming [15, 18-20].

With the thermochemical model and the anode-hole injection model both in need of improvement, it was proposed that hole trapping at a defect-precursor site can reduce the bond-breaking activation energy in the thermochemical model. This effectively marries the two models [21]. This idea was further developed by McPherson et al. who proposed that hole-trapping can also occur at stretched (weakened) Si-O bonds so that defect creation is no longer reliant on oxygen vacancy defect sites [22, 23].

Lastly, the hydrogen release model posits that electrons reaching the anode can cause hydrogen to be released from passivated interface defects. The released hydrogens drift/diffuse across the oxide layer and form defects upon encountering certain defect precursors [24-26]. The released hydrogen could be a proton [27] or a neutral atom [28]. If it were a proton, then it can act like a hole and the activation energy lowering mechanism discussed above also works [21-23].

It was theoretically shown that electron-trapping at defect-precursor states can also lower the bond-breaking activation energy [29]. It is argued that the most suitable defect-precursor state in this model is the Si-O bond stretched due to strain. As strain increases toward the SiO_2/Si interface due to thermal expansion coefficient mismatch, the density of these stretched bonds is estimated to reach as high as $5 \times 10^{19}/cm^3$ when the SiO_2 is grown on SiC [30]. Calculation shows that trapping two electrons at these sites is even more effective in promoting bond-breaking by the electric field [31, 32].

Si-O is a strong bond and directly breaking it is difficult. The common thread of the above proposed mechanisms is that defect creation under electrical stress is aided by charge-trapping at defect-precursor sites with weakened bonds. Initially, the most popular precursor site suspected was the oxygen vacancy [9, 21, 22], but its concentration is in the $10^{11}/cm^3$ to $10^{12}/cm^3$ range for good quality gate oxides [33], which is clearly many orders of magnitude too low. The precursor concentration issue is likely one of the reasons driving the convergence of various models toward the stretched Si-O bonds (by strain) [23, 29-32]. However, even the $5 \times 10^{19}/cm^3$ estimation (from the SiO_2/SiC system which is known to have higher defect density) [30, 32] is two orders of magnitude too low to explain the success of the percolation model. In addition, the high density of stretched bonds is expected to exist only near the SiO_2/substrate interface (glassy network). This means defect creation will not be random in location, as required by the percolation model.

It was proposed that defect site with trapped electron tends to promote defect precursor formation nearby, increasing the total available precursor sites [32]. While it may solve the precursor depletion problem, this proposal breaks the randomness requirement of the percolation model.

It is generally thought that only a weakened bond (state with energy level inside the SiO_2 bandgap) can trap a charge. The problem is to find defects that distribute uniformly throughout the oxide with a sufficiently high density. In this work, it is proposed that without a defect or defect precursor state, transient hole-trapping still occurs and it can break a normal Si-O bond without the help of an externally applied electric field.

The new model

In the proposed new breakdown model, every oxygen atom in the SiO_2 film is a potential site for defect creation under electrical stress. As a hole travels across the oxide film, it transiently localizes at the oxygen lone-pair state, leading to transient local distortion of the Si-O bond associated with the oxygen atom. This distortion is a direct result of the localized positive charge repelling the silicon atoms that are also positively charged due to the polar nature of the Si-O bond. The weakened bond has a greatly increased rate of breaking.

It is well-known that hole mobility in SiO_2 is very poor [34], and the reason for this poor mobility is that the top of the SiO_2 valence band is the O $2p_\pi$ non-bonding orbital (lone-pair state) [35-38]. These non-bonding orbitals are highly localized to the oxygen atom. When a hole travels along the top of the valence band, it is a highly localized wavefunction in the form of a small polaron, meaning that it distorts the surrounding bonds and becomes self-trapped. The small polaron can still move by hopping, but the mobility is very low (2×10^{-5} cm^2/Vs at 298K) [34, 39]. Note that this self-trapping is relatively shallow because it does not remain localized for long enough to undergo the multi-phonon relaxation that results in the deeply self-trapped hole commonly referred to in the literature [40].

Figure 1a illustrates the bond distortions associated with a small polaron when there is no external applied field. The positive charge on the bridging oxygen repels (blue arrows) the silicon atoms, which are positively charged due to the polar

nature of the Si-O bond. It also attracts (red arrows) the back-bonded oxygen atoms. The result is a somewhat flattened tetrahedral Si≡ structure. Fig. 1b illustrates, qualitatively, the situation when an applied field is present (big light blue arrow). The system becomes asymmetric with the field of the positive charge aligns with the applied field on one side and against it on the other. Naturally, the forces are strengthened on the side with the aligned field (bigger arrows) and weakened on the other side (smaller arrows). Of course, the ≡Si-O-Si≡ orientations in the amorphous SiO_2 film are random and should be accounted for. With weakened strength, the bond between the silicon atom and the bridging oxygen atom become easier to break to form a non-bridging oxygen hole center (NBOHC), and a positively charged E'-center where the Si≡O structure (fig. 1c) is nearly planar [41]. The positive charge on the *E'* center will quickly detrap and the nearly planar Si≡ structure relaxes back to the tetrahedron shaped with a dangling bond (fig. 1d).

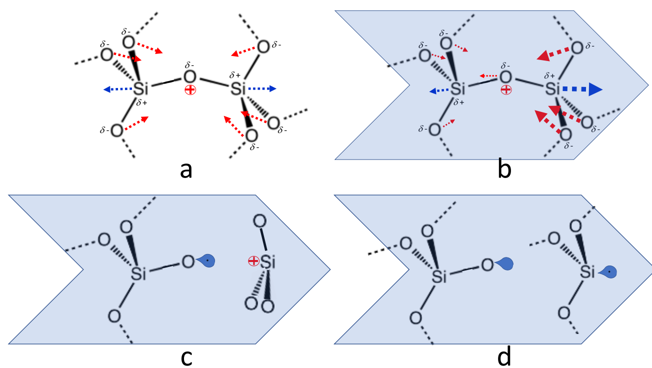

Figure 1 a: A hole is localized at the lone pair state of the bridging oxygen atom of the ≡Si-O-Si≡ structure. The positive charge repels (broken blue arrows) the silicon atoms with partial positive charge due to the polar nature of the Si-O bond. It also attracts (broken red arrows) the back-bonded oxygen atoms. b: In the presence of an applied field (big light blue arrow) the system becomes asymmetric. The silicon atom on one side is pushed further away from the bridging oxygen atom (big broken blue arrow) while the silicon atom on the other side feels a suppressed repulsion (small broken blue arrow). Similar asymmetric forces are felt by the back-bonded oxygen atoms (broken red arrows). c: The Si-O bond on the side of enhanced stretching becomes easier to break, ending up with a positively charged *E'* center with flattened Si≡ structure, and a non-bridging oxygen hole center (NBOHC). d: The positive charge rapidly detraps and the resulting Si≡ structure relax back to a tetrahedron with a dangling bond.

In the absence of an applied field

We first examine the trapping of a hole at the bridging oxygen atom without considering the externally applied electric field. Before any hole capture, the polar nature of the Si-O bond means that there is a net partial negative charge on the oxygen atom and a net partial positive charge on the silicon atoms. In a SiO_2 network, the excess partial charge on various atoms is difficult to calculate. Using machine learning to improve the accuracy of the empirical interatomic potentials, Novikov *et al*. calculated the partial charges of SiO_2 network with reduced uncertainty [42]. They found that the partial charge on the oxygen atom is –0.48 while the partial charge on the silicon atom is +0.96. When the bridging oxygen atom localize a hole, it gains a +1.0 charge, or has a +0.52 net charge.

Using semiempirical molecular orbital methods applied to finite clusters of atoms, Edwards [43] found the excess charge on the oxygen atom is +0.424 after trapping a hole, smaller than the +0.52 value before trapping a hole. Given that the calculation does not include long range Coulombic interactions (implicit given the small clusters), this is likely less accurate than Novikov *et al*'s approach. One can conclude that trapping a hole hardly change the charge distribution. Even though the trapped hole would attract more negative charges from the Si-O bond, the effect is very small. It is likely because pulling electrons from the bond disturbs not just that bond but the whole already highly polar network.

Thus, the trapping of a hole on the bridging oxygen atom produces a repulsion between a full positive charge and a nearly full (+0.96) positive charge on the silicon atom.

The repulsion energy can be calculated from the potential energy (as seen by a test charge, *q*) of a point charge as a function of distance:

$$P = \frac{1}{4\pi\epsilon_0}\frac{q_1 q_2}{r\epsilon} = 0.37eV/nm \qquad (1)$$

Where ε_0 is the dielectric constant of vacuum, $\varepsilon = 3.9$ is the relative dielectric constant of SiO_2, *r* is the distance between the two charges. Thus, the repulsion energy is 1 x 0.96 x 0.37=0.355 eV/nm. The repulsion energy as a function of separation (longer bond length) is shown in figure 2. Note that the goal is to find the additional repulsive potential when a hole is localized on the bridging oxygen, we therefore concern only the increase (from equilibrium) in positive charge on the bridging oxygen and how it repels the total (not just the increase) excess positive charge on the silicon atom.

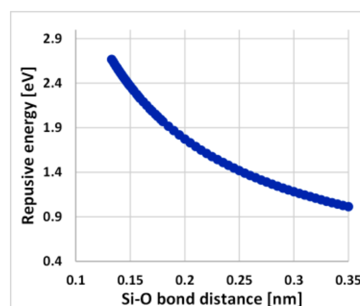

Figure 2 The localized hole changes the distribution of the electron of the polar Si-O bonds. An increase in positive charge happens on both the bridging oxygen and the silicon atoms. The repulsive potential felt by the silicon atom as a function of Si-O bond distance is shown.

The repulsion energy modifies the potential energy between the bridging oxygen atom and the silicon as a function of bond length by adding to it. Using the extended Mie-Grüneisen molecular model of McPherson [23], we get the potential-bond

length relationship shown in figure 3 (Blue curve). To produce the blue curve in figure 3, the approach in [23] has been followed exactly. So, it is not detailed here. The repulsive energy of figure 2 is added to the blue curve to produce the red curve which is the potential-bond length relationship after the localization of a hole on the bridging oxygen atom.

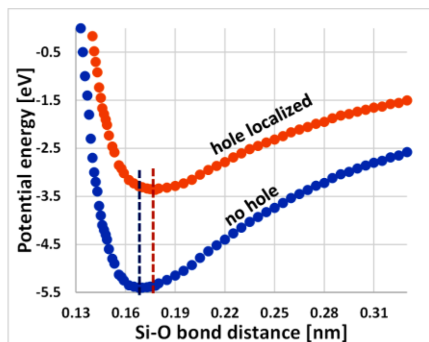

Figure 3 The blue curve is the potential-location curve of the Si-O based on the extended Mie-Grüneisen molecular model of McPherson [23]. The orange curve is when the repulsion of the silicon atom by the localized hole on the bridging oxygen atom is added. The repulsion raises potential and reduces the bond energy as expected.

Intuitively, the repulsive energy destabilize the bond and it is reflected by a much shallower potential well. The Si-O bond length is increased by 0.008 nm or stretched by 4.7%, in agreement with the 0.009 nm from *ab initio* calculation [43]. The potential minimum, or the bond energy, is reduced from -5.4 eV to -3.3 eV, a reduction of 2.1 eV.

To break the stretched O-Si bond, the Si atom must move sufficiently away from the bridging oxygen atom. McPherson argued that the silicon atom must move beyond the plane of the three oxygen atoms back bonded to the silicon [23, 44]. To do so, there is another barrier to overcome: Flipping the Si≡O structure.

Following McPherson [23] again, one can calculate the potential energy between the silicon atom and the three back-bonded oxygens in the absence of the localized hole. Fig. 4 shows the potential energy (blue curve, left scale) which goes through a maximum, associated with the point of flipping the Si≡O structure. This energy bump must be felt by the silicon atom as it moves away from the bridging oxygen. Since at the equilibrium position, the effect of all four bonds must be fully balanced, we can set the value at 0.17nm to zero. Only the variation from the equilibrium point (red curve, right scale) will affect the Si-O bond position-energy curve.

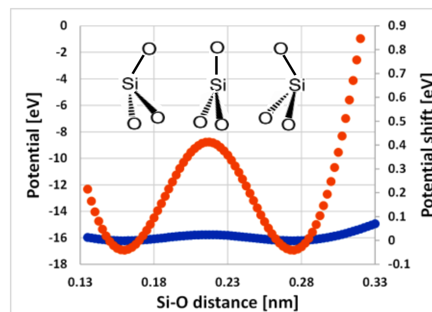

Figure 4 The blue curve (left vertical scale) is the potential energy of the three back Si-O bonds when the silicon atom is moved from one end of the tetrahedron through the center to the other end of a flipped tetrahedron. The oxygen atoms are assumed to be fixed in space. The red curve (right vertical scale) is the change in potential of the Si-O bond with the bridging oxygen. The potential at equilibrium bond length is use as zero to emphasize the changes experienced by the silicon atom as it moves.

After adding this energy variation to the potential curve with the localized hole, we end up with a potential curve that has a plateau from 0.25 nm to 0.28 nm, a location beyond the plane of the three back-bonded oxygen atoms (fig. 5, blue plot). At this bond distance, the Si-O bond is broken.

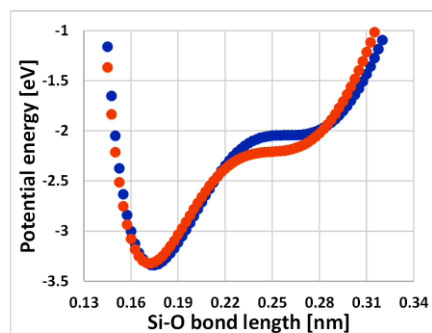

Figure 5 The blue curve is the potential-location curve of the Si-O bond after the additional potential involve in flipping the Si≡ structure to ≡Si as the silicon atom is pushed further and further away from the bridging oxygen. The red curve is when the attraction between the bridging oxygen atom and the three back-bonding oxygen atoms are accounted for. The attraction tends to help the flipping process and therefore lowers the additional barrier involve in the flipping.

In the presence of a localized hole, the electrostatic field pushes the silicon atom away (fig. 1a) while also attracts the back-bonded oxygen atoms. Thus, the O-Si-O bonding angle must reduce which also weaken the Si-O back bonds. This has the effect of lowering the barrier of flipping the Si≡O structure. To account for these additional factors, the plane of the three back-bonding oxygen atoms is moved closer to the silicon (flattening the Si≡O structure) by 17% in the calculation. The result is the red curve in fig. 5. A decrease in barrier results as expected. However, this decrease is small, and it make sense because the entire potential change for flipping the Si≡O structure is only 0.4 eV (fig. 4).

The significance of the potential plateau is that once the barrier is overcome, there is no resistance to further stretch the Si-O

bond from 0.23 nm to 0.27 nm – a length at which the covalence nature of the bond is destroyed. Furthermore, the flipping of the Si☰O structure means achieving the state depicted in fig. 1c.

With the applied field

Fig. 1b illustrates a qualitative picture of the effect of an external applied field. That figure is redrawn in fig. 6 to emphasize the effect of an external field *after* a hole is stabilized on the bridging oxygen atom.

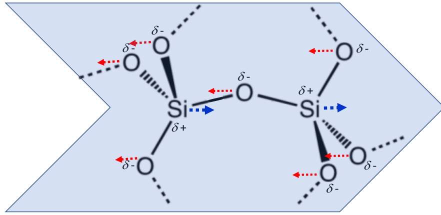

Figure 6: Fig 1b redrawn to high light the applied field's effect on the atoms *after* they have equilibrated with a trapped hole.

The bridging oxygen atom is pushed by the field to the left while the left silicon atom is being pushed to the right. This results in the compression of the Si-O bond, which is prohibited by the steep energy rise. The right-hand side silicon atom will be pushed away from the bridging oxygen atom. As the silicon atom moves, it gains energy ε from the Lorentz field (due to external field) by

$$\varepsilon = \delta_{Si} E_{lo} \delta_r \qquad (2)$$

where δ_{Si} is the excess positive charge on the silicon atom, E_{lo} is the Lorentz field and δ_r is the distance the silicon atom moves. The energy gain of the silicon atom moving from the equilibrium positive can be added to the bond's potential-position curve as reduction in potential. The result is shown in fig 7 for external field from 1MV/cm to 9 MV/cm.

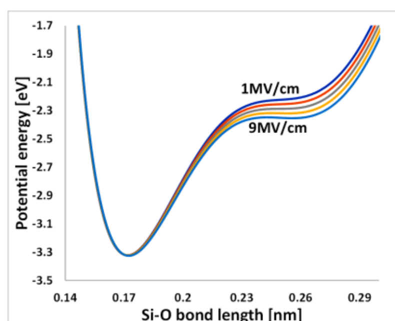

Figure 7 In the effect of an applied field on the Si-O bond's potential-position curve is very small.

The effect of the applied field is relatively small. This may be surprising to those who are familiar with the E model [9, 22, 23]. However, when considering that the field from a trapped charge at short distances is much larger than most externally applied fields, it starts to make sense.

The torque exerted by the applied field on the dipole moment associated with the Si☰O structure has the tendency to flatten the structure and help further lower the barrier. However, as we have seen from fig. 5, this barrier lowering is small even under the field of the localized hole, it can be neglected when most of the values considered here are approximations.

Altogether, the localization of a hole at the lone-pair state of the oxygen atom lowers the bond-breaking barrier from 5.4 eV (fig. 3) to 1.1 eV @ 1MV/cm and 0.97 eV @ 9MV/cm (fig. 7). This establishes that the localization of a hole at the bridging oxygen atom weakens the strong Si-O bond enough so that it can be broken. However, the role of the applied field is not to significantly lower the barrier, but instead to greatly increase the steady state concentration of the trapped holes (which increases the bond-breaking rate).

After showing how the Si-O bond can be broken, most modeling efforts would consider the job complete [9, 21, 22, 23, 29, 31, 32, 44]. However, the potential-location curves shown in fig. 7 and similar curves in other models suggest that when the trapped charge is gone, the broken bond will heal itself rapidly. This is not in agreement with the experimental fact that defects created by electrical stress are very difficult to anneal [45]. Hence, an additional process must occur to make the bond-breaking process far more stable. It is argued here that the positive charge located at the silicon in fig. 1c is rapidly detrapped and the flattened Si☰O structure, which is sp^2 hybridized, would relax back to a tetrahedron – the preferred sp^3 hybridization of silicon atom as shown in fig. 1d.

The reason the positive charge on the silicon will rapidly detrap can be found from fig. 8 where the Si-O bond potential-location curves after the localization of a hole and at the presence of applied fields are plotted together with the SiO_2 band diagram. (Note, the energy scale is from theory [35-38] which often gets 8 eV bandgap, not the experimental value.) The pristine Si-O bond potential-location curve is also shown for reference. As shown, the broken Si-O bond (bond length > 0.23 nm) with a positive charge is at an energy level very close to the SiO_2 valence band edge for all applied field conditions, indicating that the positive charge will quickly move away toward the cathode direction.

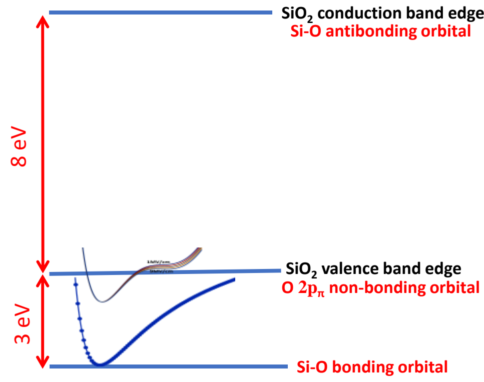

Figure 8 The calculated potential-location curve for the Si-O bond (Thick blue curve) and the curves after the localization of a hole at the bridging oxygen atom and the presence of applied fields (thinner curves) are plotted along with the theoretical band edges. The bottom of the thick blue curve is the Si-O bonding orbital which is 3 eV below the valence band edge of SiO_2. With the localized hole and the applied field, the stretched (broken) Si-O potential is very close to the valence band edge.

Not only the positively charged *E*' center will lose the charge and relax, but the non-bridging oxygen hole center (NBOHC) will also relax. Afterall, the constraint of the Si-O bond is no longer there. With both structures relaxed, bringing them back together is naturally more difficult because there is a high barrier. Thus, the bond-breaking process is irreversible at operating temperatures. A high-temperature anneal is needed to remove the created E'-center, consistent with experiments.

The Kinetics of breakdown

The bond-breaking mechanism discussed so far relies on the transient localization of a hole on the oxygen atom. The emphasis here is transient: everything happens during the very brief time the hole resides on the oxygen atom. It is not commonly thought that holes have a highly mobile nature in SiO_2. However, even with a mobility of 2 x 10^{-5} cm^2/Vs, it takes less than 1 ms to drift-diffuse through a 1 μm thick oxide film as demonstrated by Hughes [39]. For "thick" gate oxide in the 10s of nm, the resident time is in μs or less. Thus, the bond-breaking process is in competition with the hole-hopping process. This complexity can be ignored by realizing that the bond-breaking process is dependent on the steady-state hole concentration, C_h, in the oxide film. As the steady state concentration of holes is inexhaustible, defect creation becomes a zeroth order process. One can write the defect creation rate as,

$$\frac{dC_D(t)}{dt} = kC_h \qquad (3)$$

where C_D is defect density, k is the rate of breaking the bond weakened by the localized hole and is given by the Eyring–Polanyi equation,

$$k = \frac{k_B T}{h} exp\left(\frac{-\Delta E_a}{\frac{k_B T}{q}}\right) \qquad (4)$$

$$=3.93 \times 10^{11} \times \frac{T}{300} e^{-300*\Delta E_a/(0.026*T)}$$

where E_a is the bond-breaking barrier in *eV* shown in fig. 7, k_B the Boltzmann constant, *T* is temperature in Kevin, *h* is Plank's constant.

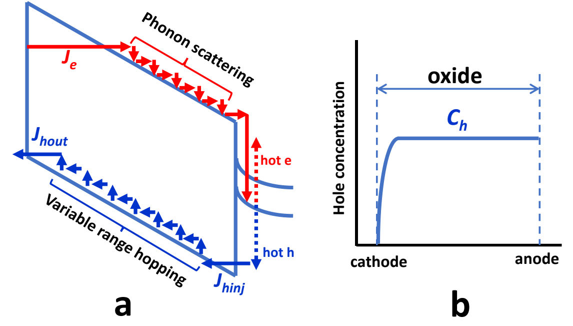

Figure 9 a: Illustration of the anode-hole injection. Electrons tunnel into the SiO_2 conduction band with a fluence of J_e. The electrons gain energy from the electric field but lose energy by phonon scattering until it reaches very close to the anode where it gains substantial energy from a potential drop. The energetic electrons produce hot electrons and hot holes through impact ionization in the substrate. The hot hole back tunnel into the oxide with a fluence J_{hinj}. It travels toward the cathode as small polarons via variable range hopping and finally tunnel into the cathode with a fluence J_{hout}. b: The steady state hole concentration, C_h, in the oxide film from cathode to anode. It is uniform through most of the oxide thickness and drop rapidly near the cathode.

The main source of hole is the anode-hole injection mechanism. Figure 9 illustrates the hole injection process. Electrons tunneling into the oxide conduction band with a fluence J_e. They gain energy from the field but lose it by phonon scattering. Reaching the anode, the potential drop gives the electrons enough energy to cause impact ionization in the substrate. Hot electrons and holes are created and the hot holes tunnel back into the oxide film with a fluence J_{hinj}. Holes transport across the oxide with a drift-diffusion velocity *v* and flow out of the oxide film to the cathode with a fluence J_{hout}. At steady state,

$$J_{hin} = J_{hout} = C_h v \qquad (5)$$

which can be rewritten as,

$$J_e \alpha T_h = C_h \mu_h E \qquad (6)$$

or

$$C_h = \frac{\alpha T_h}{\mu_h} \frac{1}{E} J_e \qquad (7)$$

where J_e is the electron fluence arriving at the anode, α is the hot hole creation efficiency (impact ionization coefficient), and T_h is the probability of the hole tunneling back into the oxide, C_h is the hole concentration in the oxide, and μ_h is the hole mobility.

For thick oxides, electrons arrive the anode with approximately the same energy regardless of the applied field (fig. 9a). Thus both α and T_h are independent of field. There is also a well-established constant C_h region in the oxide film (fig. 9b). J_e is

given by the well-known Fowler-Nordheim (FN) tunneling equation [46],

$$J_e = K_A E^2 exp(-K_B/E) \quad (8)$$

where, for electron injection barrier ϕ_B = 3.1 eV,

$$K_A = \frac{q^3 m}{8\pi h m_{OX} \emptyset_B} = 1.25 \times 10^{-6} \left(\frac{A}{V^2}\right)$$

$$K_B = \frac{4\sqrt{(2m_{OX})}}{3\frac{h}{2\pi}q} {\emptyset_B}^{3/2} = 2.335 \times 10^8 \left(\frac{V}{cm}\right)$$

with m being free electron mass, m_{OX} = 0.43m being effective electron mass in the oxide.

Combining (3), (7) and (8), we get,

$$\frac{dC_D(t)}{dt} = kK_C C_h = kK_C \frac{\alpha T_h}{\mu_h} K_A E e^{-K_B/E} \quad (9)$$

as the defect creation rate. A constant K_C is added to reflect that only some ΞSi-O-SiΞ are aligned with the applied field.

From fig. 7, we can see that the bond-breaking barrier is largely independent to the applied field E. We can use (4) for k and set K_C = 1, we get

$$\frac{dC_D(t)}{dt} = K_A \frac{\alpha T_h}{\mu_h} \frac{k_B T}{h} E e^{-(\frac{K_B}{E} + \frac{q\Delta E_a}{k_B T})} \quad (10)$$

or

$$\frac{dC_D(t)}{dt} = K_{all} E e^{-\frac{K_B}{E}} \quad (11)$$

where $$K_{all} = K_A \frac{\alpha T_h}{\mu_h} \frac{k_B T}{h} e^{-\frac{q\Delta E_a}{k_B T}}$$

Equation (11) is the main result of the new model. It gives the defect creation rate as a function of the electric field. To compare its prediction with experimental data in the literature, it needs to be written in the form of time to breakdown. We write,

$$C_{DC} = T_F \frac{dC_D(t)}{dt} \quad (12)$$

where C_{DC} is the critical defect density to breakdown, T_F is time to breakdown. Rearranging (11) and (12), we get,

$$T_F = \frac{C_{DC}}{kC_h} = \frac{C_{DC}}{K_{all} E e^{-\frac{K_B}{E}}} \quad (13)$$

and

$$ln\, T_F = ln\, C_{DC} - ln\, K_{all} - ln\, E + \frac{K_B}{E} \quad (14)$$

The middle form of (13) emphasize the role of hole concentration when the barrier (therefore k) is constant. An experiment [18] found that at 8MV/cm stress of 25 nm oxide, a flat band shift of ~ 1V resulting from hole-trapping, which translates to a steady-state hole concentration, C_h, of ~1 mC/cm^3, or ~10^{16}/cm^3. The k term, according to (4) for barrier height of 0.98eV (fig. 7), is 1.7 x 10^{-5}. We therefore have, at 8MV/cm,

$$T_F \approx \frac{C_{DC}}{2 \times 10^{11}}$$

If the critical defect density is 1 x 10^{19}/cm^3 (for capacitor size of 10^{-3}cm^2), it takes 5 x 10^7 seconds to break. This is reasonable for breakdown that has not been shortened by extrinsic defects. Thus, this numerical example illustrates that the Si-O bond weakening by a localized hole can indeed be sufficient to produce a bond breaking rate commensurate with experiment.

Experimental data usually plot lnT_F versus E or *1/*E. If we differentiate *ln(*T_F*) w. r. t. E*, equation (14) should give,

$$slope = -\left(\frac{K_B}{E^2} + \frac{1}{E}\right) \quad (15)$$

If we differentiate *ln(*T_F*) w. r. t.* 1/*E*, equation (14) should give,

$$slope = K_B + E \quad (16)$$

Fig. 10 plots the calculated slope for *1/E* dependent (fig. 10a) case and *E* dependent (fig. 10b) case, along with many reported experimental values from the literature [47-61].

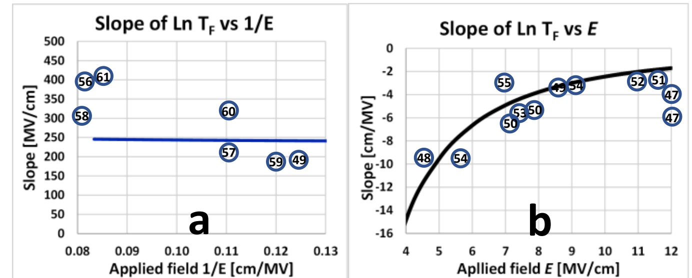

Figure 10 Predicted slopes for plotting lnT_F vs 1/*E* (a) and vs *E* (b). Circles with enclosed number are extracted data from literature (number is the reference) [47-61]. Each experimental value is extracted from a range of field. The middle of that range is used as the X coordinate.

Note that experimental values scatter significantly, reflecting the quality variation of the oxides under study. Additionally, most experiments did not have good enough statistics to extract reliable slopes. Given that, the predicted slopes are in reasonable agreement with experiments. Note that equations (15) and (16) have no fudgeable quantities. The combination of a reasonable predicted breakdown time and field acceleration is a strong statement to the correctness of the model that oxide breakdown is driven by the steady state hole concentration.

For the E dependent cases, the predicted slope varies significantly with applied field. However, most experiments are done within a narrow range (7 MV/cm to 10 MV/cm) of field, so observing an apparent constant slope is reasonable.

For thick oxides, the terms that make up C_h in (7) are largely temperature independent, except μ_h which increase with temperature. Being a variable range hopping mechanism, this temperature dependent mobility can be express as [62],

$$\mu_h = \mu_{h0} e^{-\left(\frac{T_0}{T}\right)^{1/4}} \tag{17}$$

which is a relatively weak function. Here, μ_{h0} is the hole mobility at T_0. However, it will still reduce the temperature effect by counter-acting (high mobility means lower hole concentration and slower defect creation) the increase in bond-breaking rate. It will increase the extracted activation energy from experimental data.

When the gate oxide is thin, electron injection changes from FN tunneling to direct tunneling. The energy of the electron arriving at the anode is directly linked to the applied voltage. The impact ionization coefficient, α, drops exponentially with the electron energy. Simultaneously, the hot hole energy also drops, causing the hole tunneling probability to decrease exponentially as well. Thus, the J_{hinj} drops exponentially with applied voltage, so will C_h. In addition, when the gate oxide is thin, the variable range hopping process breaks down as more holes tunnel directly to the cathode and the effective mobility becomes larger. For very thin gate oxides, part, if not all, of the thickness is in this regime and C_h is effectively smaller. The combined effect of direct tunneling, exponential decreasing J_{hinj} with applied voltage, and the increase in effective mobility is that the defect creation rate becomes a strong function of the applied voltage and that the defect creation per injected electron drops exponentially with the applied voltage. This matches experimental observations [63, 64].

Not all hole transport through the oxide can cause defect generation. Holes that tunneling directly across, such as hole tunneling injection from p-FET with ultra-thin gate oxide, would not produce defect. Only those that transport along the top of the oxide valence band as small polaron will produce defect. For the p-FET with thin oxide case, electron tunneling in the opposite direction can produce hot hole that transport at the top of the valence band. Degradation still occurs, but at a slower rate.

Further discussions

The above analysis shows that the movement of holes in the oxide as a small polaron can greatly increase the probability of Si-O bond breaking without invoking any defect-precursors, and the time to failure slope is reasonable comparing to experiments. In the discussion of the hydrogen release model earlier, we pointed out that if the released hydrogen is a proton, it can act like a hole, and the model established here may also apply. However, there is a big difference between injected holes and released protons. Injected holes are an inexhaustible source while released hydrogen is a limited source. For the hydrogen release model to work, the released hydrogen must be able to drift-diffuse and only the steady state concentration will support bond-breaking by lowering the barrier. Only a small fraction of the limited released hydrogen is effective. There will quickly be a hydrogen source depletion problem.

While it is argued here that defect creation leading to breakdown must not rely on preexisting defects or defect-precursors, it does not mean that they do not cause bond-breaking. They just don't have sufficient density to be the main cause of breakdown. Some defects or defect-precursors can speed up the breakdown process by locally increasing the electron fluence via trap-assisted-tunneling (TAT) if they happen to have the right energy level and are located at the right distance from the interface. However, this faster breakdown mechanism is not uniform. It will cause the breakdown distributions to have Weibull slopes deviating from the percolation model, as demonstrated recently [65, 66].

Note that while the model discussion focuses on SiO_2, the physics is not unique to SiO_2. Indeed, it applies to any charge transport through dielectric in the form of small polaron. This clearly include, but not limit to, most oxides.

Note also that while majority of holes transiting the oxide at the top of the valence band as small polarons, some will be trapped at existing defect sites (hole-traps). These hole-trapping processes are too low in concentration to be the cause of breakdown, but are responsible for phenomena such as bias-temperature-instability.

Conclusions

In summary, a new gate oxide breakdown model is proposed. It does not rely on any pre-existing defect or defect-precursor. Instead, all the oxygen atom sites in the SiO_2 system can be the bond-breaking site. Thus, the problem that plagues all previous gate oxide breakdown models, namely precursor depletion, is resolved. Holes traversing the oxide film as small polarons are the culprit. They transiently localize at the lone pair state of bridging oxygen atoms and weaken the Si-O bonds to drastically increase the probability of the bonds being broken over time. The role of the external applied field is mainly to increase the steady state hole concentration in the oxide film, not to speed up bond breaking through barrier lowering.

References

[1] Lombardo, S., Stathis, James H., Linder, Barry P., Pey, Kin Leong, Palumbo, Felix, Tung, Chih Hang, "Dielectric breakdown mechanisms in gate oxides." J. Appl. Phys. **98**(12): 121301(2005).

[2] Harari, E., "Dielectric breakdown in electrically stressed thin films of thermal SiO2." J Appl. Phys. **49**(4), 2478(1978).

[3] Nissan-Cohen, Y., Shappir, J., Frohman-Bentchkowsky, D., "Trap generation and occupation dynamics in SiO2 under charge injection stress." J. Appl. Phys. **60**(6): 2024(1986).

[4] Avni, E. and J. Shappir, "A model for silicon-oxide breakdown under high field and current stress." J Appl. Phys. **64**(2): 743(1988).

[5] Suñé, J., Placencia, I., Barniol, N., Farrés, E., Martín, F., Aymerich, X., "On the breakdown statistics of very thin SiO2 films." Thin Solid Films **185**(2): 347(1990).

[6] Dumin, D. J., Maddux, J. R., Scott, R. S., Subramoniam, R., "A model relating wearout to breakdown in thin oxides." IEEE Trans. Electron Dev.,_ **41**(9), 1570(1994).

[7] Degraeve, R., Groeseneken, G., Bellens, R., Depas, M., Maes, H.E., "A consistent model for the thickness dependence of intrinsic breakdown in ultra-thin oxides." IEEE Int. Electron Dev. Meeting, pp863, 1995.

[8] Stathis, J. H., "Percolation models for gate oxide breakdown." J Appl. Phys. **86**(10), 5757(1999).

[9] McPherson, J. W. and H. C. Mogul, "Underlying physics of the thermochemical E model in describing low-field time-dependent dielectric breakdown in SiO2 thin films." J. Appl. Phys. **84**(3): 1513(1998).

[10] Kimura, M., "Field and temperature acceleration model for time-dependent dielectric breakdown." IEEE Trans. Electron Dev. **46**(1): 220(1999).

[11] Haddad, S. and L. Mong-Song, "The nature of charge trapping responsible for thin-oxide breakdown under a dynamic field stress." IEEE Electron Dev. Lett. **8**(11): 524(1987).

[12] Schuegraf, K. F. and H. Chenming, "Hole injection oxide breakdown model for very low voltage lifetime extrapolation." IEEE Int. Reliability Phys. Symp., 1993, p7.

[13] Fischetti, M. V., "Model for the generation of positive charge at the Si-SiO2 interface based on hot-hole injection from the anode." Phys. Rev. B **31**(4): 2099(1985).

[14] Chen, I. C., Holland, S., Hu, C., "OXIDE BREAKDOWN DEPENDENCE ON THICKNESS AND HOLE CURRENT-ENHANCED RELIABILITY OF ULTRA THIN OXIDES." Int. Electron Dev. Meeting 1986, p660.

[15] Uchida, H. and T. Ajioka, "Electron trap center generation due to hole trapping in SiO2 under Fowler–Nordheim tunneling stress." Appl. Phys. Lett. **51**(6): 433(1987).

[16] Alam, M. A., Bude, J., Weir, B., Silverman, P., Ghetti, A., Monroe, D., Cheung, K. P., Moccio, S., "An anode hole injection percolation model for oxide breakdown - the 'doom's day' scenario revisited." IEEE Int. Dev. Meeting (IEDM), 1999, p715.

[17] Rasras, M., I. De Wolf, G. Groeseneken, B. Kaczer, R. Degraeve, H. E. Maes, "Photo-carrier generation as the origin of Fowler-Nordheim-induced substrate hole current in thin oxides." IEEE Trans. Electron Dev. **48**(2): 231(2001).

[18] Nissan-Cohen, Y., Shappir, J., Frohman-Bentchkowsky, D., "High field current induced-positive charge transients in SiO2." J. Appl. Phys. **54**(10): 5793(1983).

[19] Weinberg, Z. A. and T. N. Nguyen, "The relation between positive charge and breakdown in metal-oxide-silicon structures." J. Appl. Phys. **61**(5): 1947(1987).

[20] Cheung, K. P., "Efficient method for plasma-charging damage measurement." IEEE Electron Dev. Lett. **15**(11): 460(1994).

[21] Cheung, K. P., "A physics-based, unified gate-oxide breakdown model." IEEE Electron Dev. Meeting, 1999, p719.

[22] McPherson, J. W., Khamankar, R. B., Shanware, A., "Complementary model for intrinsic time-dependent dielectric breakdown in SiO2 dielectrics." J. Appl. Phys. **88**(9): 5351(2000).

[23] McPherson, J. W. "Extended Mie-Grüneisen molecular model for time dependent dielectric breakdown in silica detailing the critical roles of O–Si≡O3 tetragonal bonding, stretched bonds, hole capture, and hydrogen release." J. Appl. Phys. 99(8): 083501(2006).

[24] DiMaria, D. J. and J. W. Stasiak, "Trap creation in silicon dioxide produced by hot electrons." J. Appl. Phys. **65**(6): 2342(1989).

[25] Nissan-Cohen, Y. and T. Gorczyca, "EFFECT OF HYDROGEN ON TRAP GENERATION, POSITIVE CHARGE TRAPPING, AND TIME-DEPENDENT DIELECTRIC BREAKDOWN OF GATE OXIDES." Electron device letters 9(6), 287(1988).

[26] Conley, J. F. and P. M. Lenahan, "Room temperature reactions involving silicon dangling bond centers and molecular hydrogen in amorphous SiO2 thin films on silicon." IEEE Trans. Nuclear Sci. **39**(6): 2186(1992).

[27] Griscom, D. L., "Hydrogen model for radiation-induced interface states in SiO2-on-Si Structures: A review of the evidence." J. Electronic Mater. **21**(7): 763(1992).

[28] Blöchl, P. E. and J. H. Stathis, "Hydrogen Electrochemistry and Stress-Induced Leakage Current in Silica." Phys. Rev. Lett. **83**(2): 372(1999).

[29] Bersuker, G., Korkin, Anatoli, Jeon, Yongjoo, Huff, Howard R., "A model for gate oxide wear out based on electron capture by localized states." Appl. Phys. Lett. **80**(5): 832(2002).

[30] El-Sayed, A.-M., Watkins, Matthew B., Shluger, Alexander L., Afanas'ev, Valeri V., "Identification of intrinsic electron trapping sites in bulk amorphous silica from ab initio calculations." Microelectronic Engineering **109**, 68(2013).

[31] Gao, D. Z., El-Sayed, Al-Moatasem, Shluger, Alexander L., "A mechanism for Frenkel defect creation in amorphous SiO₂facilitated by electron injection." Nanotechnology **27**(50): 505207(2016).

[32] Padovani, A., Gao, D. Z., Shluger, A. L., Larcher, L., "A microscopic mechanism of dielectric breakdown in SiO2 films: An insight from multi-scale modeling." J. Appl. Phys. **121**(15): 155101(2017).

[33] Conley, J. F., Lenahan, P. M., McArthur, W. F., "Preliminary investigation of the kinetics of post oxidation rapid thermal anneal induced hole-trap-precursor formation in microelectronic SiO2 films." Appl. Phys. Lett. **73**(15): 2188(1998).

[34] Hughes, R. C., "Hole mobility and transport in thin SiO2 films." Appl. Phys. Lett. **26**(8): 436(1975).

[35] DiStefano, T. H. and D. E. Eastman, "Photoemission Measurements of the Valence Levels of Amorphous SiO2." Phys. Rev. Lett. **27**(23): 1560(1971).

[36] Schneider, P. M. and W. B. Fowler, "Band Structure and Optical Properties of Silicon Dioxide." Phys. Rev. Lett. **36**(8): 425(1976).

[37] Pantelides, S. T. and W. A. Harrison, "Electronic structure, spectra, and properties of 4:2-coordinated materials. I. Crystalline and amorphous SiO2 and GeO2." Phys. Rev. B **13**(6): 2667(1976).

[38] Chelikowsky, J. R. and M. Schlüter, "Electron states in alpha-quartz: A self-consistent pseudopotential calculation." Phys. Rev. B **15**(8): 4020(1977).

[39] Hughes, R. C., "Time-resolved hole transport in SiO2." Phys. Rev. B **15**(4): 2012(1977).

[40] Griscom, D. L., "Self-trapped holes in amorphous silicon dioxide." Phys. Rev. B **40**(6): 4224(1989).

[41] Griscom, D. L., "E' center in glassy SiO2: 17 O, 1 H, and "very weak" 29 Si superhyperfine structure." Phys. Rev. B **22**(9): 4192(1980).
[42] Novikov, Ivan S., Shapeev, Alexander V., “Improving accuracy of interatomic potentials: more physics or more data? A case study of silica.” https://doi.org/10.48550/arXiv.1808.03783
[43] Edwards, A. H., “Theory of the Self-Trapped Hole in a-SiO_2,” Phys. Rev. Lett. **71**(19), 3190(1993).
[44] McPherson, J. W., “Quantum Mechanical Treatment of Si-O Bond Breakage in Silica Under Time Dependent Dielectric Breakdown Testing.” IEEE Int. Reliability phys. Symp., 2007, p209.
[45] Pantisano, L. and K. P. Cheung, "Stress-induced leakage current (SILC) and oxide breakdown: are they from the same oxide traps?" IEEE Trans. Device & Materials Reliab. **1**(2): 109(2001).
[46] Sanchez, J. J. and T. A. DeMassa, "Modeling gate emissions: A review—Part I." Microelectronic Engineering **20**(3): 185(1993).
[47] Swartz, G. A. "Gate oxide integrity of NMOS transistor arrays." IEEE Trans. Electron Dev. **33**(11): 1826(1986).
[48] Boyko, K. C. and D. L. Gerlach “Time dependent dielectric breakdown at 210A oxides.” Int. Reliability Phys. Symp., 1989.
[49] Prendergast, J., J. Suehle, P. Chaparala, E. Murphy, M. Stephenson “TDDB characterization of thin SiO2 films with bimodal failure populations.” Int. Reliability Phys. Symp. 1995.
[50] Schlund, B. J., Suehle, J., Messick, C., Chaparala, P. "A new physics-based model for time-dependent Dielectric breakdown." Microelectronics Reliability **36**(11): 1655(1996).
[51] Vincent, E., N. Revil, C. Papadas, G. Ghibaudo, “Electric field dependence of TDDB activation energy in ultrathin oxides.” European Symp. Reliability of Electron Dev., Failure Phys. and Analysis, 1996.
[52] Kimura, M. “Oxide breakdown mechanism and quantum physical chemistry for time-dependent dielectric breakdown.” Int. Reliability Phys. Symp. 1997
[53] Suehle, J. S. and P. Chaparala, "Low electric field breakdown of thin SiO2 films under static and dynamic stress." IEEE Trans. Electron Devi. **44**(5): 801(1997).
[54] McPherson, J., Reddy, V., Banerjee, K., Huy, Le, “Comparison of E and 1/E TDDB models for SiO2 under long-term/low-field test conditions.” Int. Electron Devices Meeting, 1998.
[55] Yassine, A. M., H. E. Nariman, M. McBride, M. Uzer, K. R. Olasupo, "Time dependent breakdown of ultrathin gate oxide." IEEE Trans. Electron Dev. **47**(7): 1416(2000).
[56] Ghibaudo, G., Pananakakis, G., Kies, R., Vincent, E., Papadas, C., "Accelerated dielectric breakdown and wear out standard testing methods and structures for reliability evaluation of thin oxides." Microelectronics Reliability **39**(5): 597(1999)
[57] Lee, J. C., Chen, Ih-Chin, Hu, Chenming, "Modeling and characterization of gate oxide reliability." IEEE Trans. Electron Dev. **35**(12): 2268(1988).
[58] Chen, I.-C., Holland, S. E., Chenming, Hu, "Electrical Breakdown in Thin Gate and Tunneling Oxides." IEEE J. Solid-State Circuits, 20(1): 333(1985).
[59] Shiono, N. and M. Itsumi, “A lifetime projection method using series model and acceleration factors for TDDB failures of thin gate oxides.” Int. Reliability Phys. Symp. 1993.
[60] Schuegraf, K. and C. hu, "Effects of Temperature and Defects on Breakdown Lifetime of Thin SiO2 at Very Low Voltages." IEEE Trans. Electron Dev. **41**: 1227(1994).
[61] Nafría, M., Suñé, J., Aymerich, X. "Breakdown of thin gate silicon dioxide films--A review." Microelectronics and Reliability Reliability Phys. Advanced Electron Dev. **36**(7-8): 871(1996).
[62] Mott, N. F., "Conduction in non-crystalline materials". Philosophical Magazine **19** (160): 835(1969).
[63] Nicollian, P. E., W. R. Hunter, J. C. Hu, “Experimental evidence for voltage driven breakdown models in ultrathin gate oxides.” IEEE Int. Reliab. Phys. Symp., 2000, p7.
[64] Schuegraf, K. and C. hu, "Effects of Temperature and Defects on Breakdown Lifetime of Thin SiO2 at Very Low Voltages." IEEE Trans. Electron Dev. **41**: 1227(1994).
[65] Cheung, K. P., "On the “intrinsic” breakdown of thick gate oxide." J. Appl. Phys. **132**(14): 144505(2022).
[66] Cheung, K. P., "Thick gate oxide extrinsic breakdown – The potential role of neutral hydrogen atom." Power Electronic Devices and Components **4**: 100024(2023).